Available online at www.eccomasproceedia.org
Eccomas Proceedia COMPDYN (2025) 2712-2730

ECCOMAS
Proceedia

COMPDYN 2025
10th ECCOMAS Thematic Conference on
Computational Methods in Structural Dynamics and Earthquake Engineering
M. Papadrakakis, M. Fragiadakis (eds.)
Rhodes Island, Greece, 15-18 June 2025

DISTRIBUTION IN PLAN AND ELEVATION OF DISSIPATIVE BRACING FOR SEISMIC RETROFIT OF R.C. FRAMES

Muhammad Ahmed, Piero Colajanni*, Michele Fabio Granata, Leonardo Arfeli
Department of Engineering, University of Palermo,
Viale delle Scienze, Ed. 8, 90128, Palermo, Italy.
e-mail: {muhammad.ahmed, piero.colajanni, michelefabio.granata, leonardo.arfeli}@unipa.it

Abstract

Dissipative bracing systems have been one of the approaches for improving the seismic performance of Reinforced Concrete (RC) frames in earthquake-prone areas since the 1980s. However, design methods for dissipative bracing systems are still under research. Most existing studies focus on evaluating the global stiffness and strength of the dissipative braces. At the same time, a smaller number of those define the criteria and methods for their distribution both in elevation and plan. These issues are particularly important for irregular structures, as the precise design of each brace and dissipative device must comply with local features. In this area, inadequate consideration is given to controlling the increase of axial loads in columns, which affects their deformation capacity.
Since the 1980s, seismic strengthening interventions using dissipative bracing have been developed for RC frames originally designed to withstand only gravity loads. Most of the design methods are derived based on Pushover analysis (POA), able to identify structural weaknesses at different stages under lateral displacement. However, in the literature there is an absence of retrofitting of structures designed with modern earthquake codes, in which strengthening is required due to an increase in the seismicity of the area or change in use, resulting in a change in the importance class and consequently the return period of seismic action.
In this research, criteria for the distribution of stiffnesses and resistances of dissipative bracing both in elevation and in the plan are provided, aiming at reducing structural irregularities and minimizing the reduction of column deformation capacity due to variation of the axial load.
A reinforced concrete structure is designed in a medium seismicity area according to current seismic codes using modal response spectrum analysis and a capacity design approach. POA is conducted with finite element modeling to identify structural performances and address design deficiencies. Then, due to an increment of the design seismic action, strengthening interventions by dissipative bracing are designed, using standard procedure, or based on the aforementioned criteria. Comparative evaluations through static and nonlinear dynamic analyses reveal significant improvements, including increment of deformation capacity, reduced inter-story drift demands, better stress distribution, ensuring enhanced seismic performance.

Keywords: Bracings, Retrofitting, Reinforced concrete structure, Pushover analysis

ISSN:2623-3347 Published by Eccomas Proceedia.
Peer-review under responsibility of the organizing committee of COMPDYN 2025.
doi: 10.7712/120125.12603.25518

1 INTRODUCTION

Seismic strengthening techniques exhibit significant diversity [1], as the selection of an appropriate intervention must align with the structural characteristics and inherent vulnerabilities of the system to be retrofitted [2]. Localized interventions are often sufficient for structures designed according to now outdated seismic criteria. These may include the strengthening of beams, columns [3–7], and beam-column joints [2,8,9], increases of deformation capacity in potential plastic hinge regions [10,11], enlargement of column cross-sections via jacketing [7], and the enhancement of seismic performance of non-structural elements such as infill panels [12]. The integration of the capacity to absorb seismic energy by damping devices is among the most effective solutions for both new and retrofitted structures [13–23].

If a structure exhibits inadequate lateral stiffness and isn't resistant to horizontal forces, bracing systems are historically among the most widely employed solutions [18,24–26]. Bracings equipped with hysteretic dissipative devices effectively reduce inter-story drifts and enhance energy dissipation, thereby preserving the structural frame from plasticization. The design of such bracing systems must, however, consider variation in axial loads on columns, minimizing the reduction of column deformation capacity, and corresponding increases in foundation strength, exploiting the features that stiffness and strength contributions of the bracing system can be independently controlled [27–29].

Since the 1980s, dissipative bracing design methodologies have been developed, addressing as primary design goals: i) defining performance requirements; and ii) determining the global stiffness and strength of the bracing system. Less attention has been paid to optimizing and establishing procedures in distributing stiffness and strength across the elevation and plan layout of the structure, which is particularly critical for irregular configurations, and detailing individual bracing elements and dissipative devices in accordance with specific structural attributes.

In terms of performance objectives, dissipative braces have consistently been designed to prevent plasticization of primary frame members and to mitigate damage to non-structural elements, given their inherently high stiffness and dissipation capacity [13,27,30–32]. Since the development of early methodologies [27], the non-linear static analyses, implemented by push-over analysis, and the definition of an equivalent Single Degree of Freedom (SDOF) able to capture the main features of the behavior of the whole structure, have proven to be one of the most effective techniques for determining the global stiffness and strength parameters of bracing systems, This approach is widely adopted in contemporary design procedures.

Several researchers have advanced the Direct Displacement-Based Design (DDBD) methodology [33,34] for the design of dampers. A review of retrofit design methods for RC buildings using hysteretic dampers can be found in [35].

Regarding the distribution of stiffness and strength in elevation, two predominant approaches exist: - proportional distribution based on the structural properties of the system to be retrofitted [31,36] and strategic distribution aimed at correcting elevation and plan irregularities [30,37,38].

Mazza and Vulcano [34] proposed a Displacement-Based Design (DBD) framework for dissipative bracing, ensuring inter-story drift control under seismic excitation. The approach involves proportional stiffness allocation, where in bracing stiffness is assigned relative to the unbraced frame, employing an iterative method to optimize stiffness ratios based on the frame's strength.

Bruschi et al. [18] proposed an alternative seismic upgrading methodology utilizing dissipative bracing, based on the concept of an equivalent high-damped elastic SDOF system with viscous damping and secant stiffness at the performance point. Their procedure comprises: - pushover analysis to establish the frame's capacity curve; - bilinear representation of the braced frame base shear; - top story displacement aiming at the identification of a target displacement; -

iterative determination of the equivalent viscous damping ratio and final brace stiffness/strength;
- optimization of bracing stiffness and strength distribution to match seismic demand within an acceleration-displacement response spectrum framework.

Di Cesare and Ponzo [16] introduced a methodology for designing dissipative bracing in reinforced concrete frames, using top-story displacement as the control parameter. This approach iteratively adjusts story-level stiffness and strength to regulate inter-story drift, effectively improving structural performance while avoiding excessive loading on structural elements.

Maulana et al. [39] used a genetic algorithm to optimize the location of braced restrained braces (BRB) for reinforced concrete frames with curtailed shear walls, and they found that the optimum locations of BRBs were different for each ground motion they used. Thus, a simple probabilistic method was employed to select the final locations of BRBs.

Laguardia and Franchin [40] updated a procedure [41] based on the use of the mean annual frequencies of exceedance of multiple limit states as the ingredients of an optimization function, and to carry out efficient gradient-based (constrained) optimization by using an equivalent linear model of the structure. The method was refined by presenting a member-wise reduction factor to obtain the secant stiffness of the equivalent linear model, by introducing alongside the secant stiffness of members (braces, the object of the design, and RC members, whose properties are input to the retrofit problem) also the energy dissipated used to evaluate a weighted global damping ratio of the system, and reduce accordingly the response spectrum used in the equivalent linear analysis.

Regarding the distribution of stiffness and strength in the plan, Mazza [15] proposed a displacement-based design procedure to attain a designated performance level for the in-plan least seismic capacity direction (lowest base shear among the values for all seismic input direction), with two different in plan distribution of the braces: a proportional stiffness criterion, which assumes the same position of the center of stiffness for the unbraced and braced frames at each story, and a criterion aiming at obtain the coincidence of center of mass and center of stiffness at each story, to avoid torsional response in the elastic phase, with strength distribution proportional to stiffness distribution. The results obtained by pushover analysis showed that the latter criterion provides a more uniform distribution of the vulnerability index for any direction of the seismic excitations.

Ferraioli and Lavino [17,35] refined the methodology developed by Mazza et al. [42] by incorporating capacity spectrum principles into the Displacement-Based Design (DBD) framework. Their approach addressed critical issues omitted in previous methods, such as frame-brace interaction effects leading to increased axial forces in columns and reduced ductility, torsional effects in asymmetric buildings, soft-story effects, mode shape alterations due to the transition from a Moment-Resisting Frame (MRF) to a Concentric Braced Frame (CBF). Higher mode contributions in high-rise buildings were also investigated, according to the adaptation of the Displacement-based Adaptive Pushover (DAP) method proposed by Antoniou and Pinho [43] by the capacity spectrum principles. Their procedure, validated through nonlinear time-history analysis and adaptive pushover assessments, demonstrated improved performance by optimizing damper stiffness and strength distribution along the building height, thereby achieving uniform inter-story drift. In [35] they distributed in-plan the overall story stiffness of the damped braces given to increase the torsional stiffness of the building and minimize the impact on the architectural functionality.

In [44] Ferraioli et al. developed a “two-step” pushover procedure for seismic retrofit of plan-asymmetric buildings using buckling restrained braces equipped with steel hysteretic dampers, based on the observation that conventional pushover analysis with lateral force applied at the building's center of mass may underestimate seismic torsional response. The first step involves the insertion of non-dissipative steel braces that are designed to balance the lateral stiffness

eccentricity of the structure to be retrofitted. Once the torsional effects have been mitigated, the procedure proposed by Mazza [42] can be applied.
In this research, on the basis of the findings in [17,35,44] criteria and methods for the distribution of stiffnesses and resistances of dissipative bracing both in elevation and in plan are revised, aiming at reducing structural irregularities, and minimizing the reduction of column deformation capacity due to variation of the axial load. They address the critical issues mentioned in [17], such as frame-brace interaction effects leading to variation of axial forces in columns and reduced ductility, torsional effects in asymmetric buildings, soft-story effects, and mode shape alterations. A reinforced concrete structure is designed in a medium seismicity area according to current seismic codes using modal response spectrum analysis and a capacity design approach. POA is conducted with finite element modeling to identify structural performances and address design deficiencies. Then, due to an increment of the design seismic action, strengthening interventions by dissipative bracing are designed, using standard procedure, or based on the aforementioned criteria. Comparative evaluations through static and nonlinear dynamic analyses reveal significant improvements, including increment of deformation capacity, reduced inter-story drift demands, better stress distribution, and minimized plastic hinge formation, ensuring enhanced seismic performance.

2 CAD METHOD

A simplified procedure (CAD method) proposed in [45] for design of dissipative bracing was developed based on simplified relationships, making it particularly accessible to designers. The procedure aims at providing a uniform inter-story drift along the height of the structure, ensuring a homogeneous distribution of damage in case of high seismic events and reducing the material used for bracing. The method involves a series of sequential steps, organized as shown in the flowchart in Figure (1). It begins with the characterization of the bare frame BF, then the total drift Δ_T is calculated, followed by the target eigenvector of the structure DBF structure $\varphi_{1,i} = \frac{z_i}{H_T}$. The evaluation of the target displacement is $d_{max,DBF} = \Delta_T H_T$, the mass of the corresponding SDOF is $m^* = \sum_{i=1}^{n} m_i \, z_i / H_T$, and the first-mode transformation factor is $\Gamma_1 = m^* / [\sum_{i=1}^{n} m_i \, (z_i/H_T)^2]$. A "first mode" pattern of the seismic force is used to analyze a push-over curve in order to assess the behavior of the bare frame. Then, using the equal displacement rule (with the appropriate modification factor for a stiff system having a period smaller than T_c, proposed by the seismic codes [36,46], the stiffness of the SDOF dissipative bracing system DB is designed. The equivalent vibration period of the braced frame is evaluated as T^*_{DBF},where the parameter α is defined as a function of period and is different for two different cases if $T^*_{DBF} \geq T_C$ or $T^*_{DBF} < T_C$. Then, the yield strength of the braced frame and the design parameters of the MDOF braced frame are calculated as shown in step 4.
The procedure aims to fulfill the observation in [17,35,44], regarding the procedure to determine the stiffness $k^j_{i,DB}$ and strength $V^j_{yi,DB}$ of each jth brace at the ith story distributing the total story stiffness $= k_{i,DB} = \sum_{j=1}^{nj} k^j_{i,DB}$ and the total story strength $V_{yi,DB} = \sum_{j=1}^{nj} V^j_{yi,DB}$, nj being the number of braces at the story i), taking into account the effects frame-brace interaction on the seismic force distribution along the height. Thus, the story stiffness of the bare frame is evaluated by a non-linear static analysis in which the story displacement is set equal to the target story displacement of the braced structure (i.e. obtained assuming constant inter-story drift and with zero torsional rotation); therefore, the pattern of the seismic force is the result of the analysis. Moreover, the stiffness of each brace is evaluated in order to ensure that at each story the center of stiffness of the DBF, i.e. by summing the stiffness of the frame (evaluated as described previously with those of the braces) is coincident with the center of the seismic story shear.

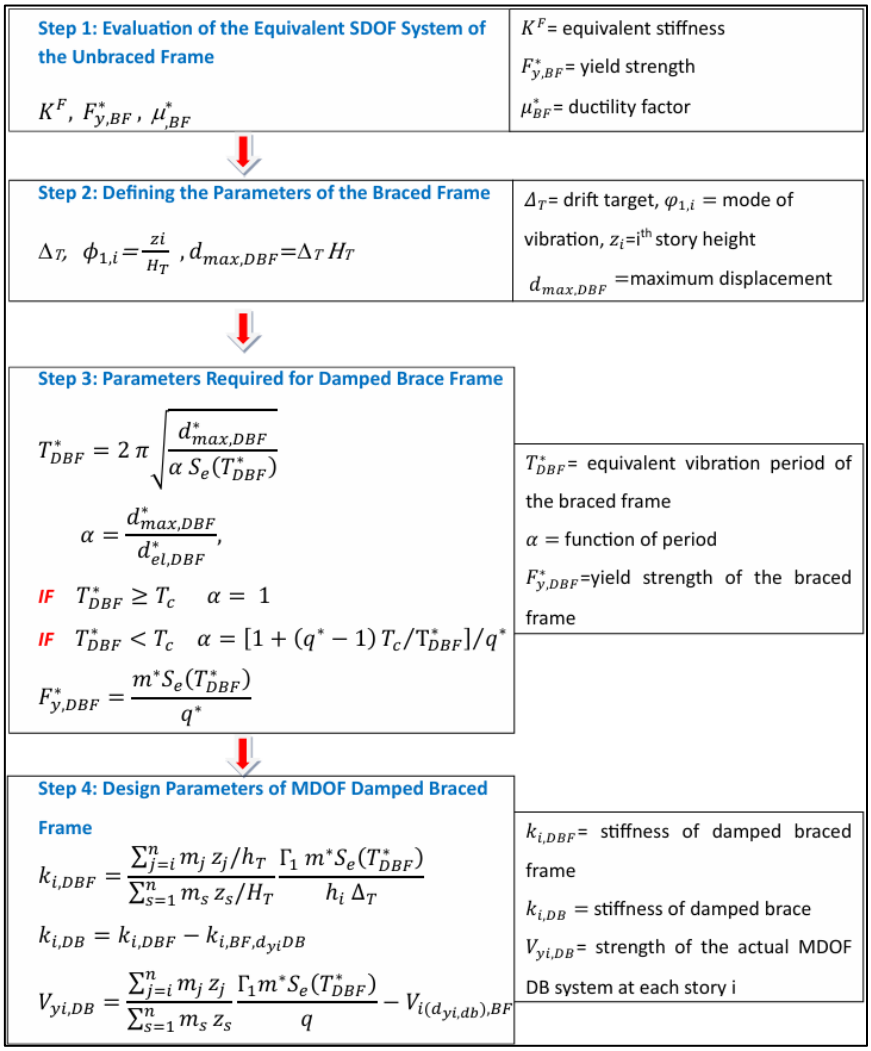

Figure 1: CAD method for design of braces [45]

In order to determine the strength of each (device of the) bracing $V^j_{yi,DB}$, an iterative procedure is performed, starting from a solution that aims at obtaining the coincidence of the center of the sum of the shear of the columns of the frame for the target configuration (i.e. evaluated with the non-linear static analysis before mentioned) and of the horizontal component of the reactions of the braces, coincident with the center of the seismic story shear, and the maximum torsional stiffness of the frame, i.e. with the stiffness of brace centrifugated as possible. Then, the effect of the axial load variation induced by the braces on the ductility of the columns is investigated, the former depending on the value of the behavior factor chosen in the design phase (steps 3 and 4 in the flowchart in Figure (1)), and position, number and strength of the braces are modified in order to obtain the smaller reduction or the largest increment of the deformation capacity of the column of the frame.

3 CASE STUDY

The above procedure is applied to the seismic upgrading of a five-story reinforced concrete frame sown in Figure (2), designed according to Italian seismic code [36] in a site with a Peak Ground Acceleration PGA=0.177 g, soil S=1.2 and dynamic amplification F_0=2.38 factors, and upper limit of the period of the constant spectral acceleration region T_c= 0.409 sec for a return period of 475 years (life safety limit state SLV). Each story has a height of 3.20 meters, and the

floor area of the first two levels is approximately 240 m^2 each, while the upper three floors are 143 m^2. The slabs are oriented in a vertical direction, and the structural G_1 and nonstructural G_2 dead loads are G_1=4.17 kN/m^2, and G_2=3.3 kN/m^2, and live load Q_k=2 kN/m^2, corresponding to seismic story weight of W_1= W_2=3226 kN, W_3= W_4=2016 kN, and W_5=1382 kN. Concrete (C25/30) with compressive characteristic strength f_{ck} = 24.9 N/mm² and B450C steel having characteristic yielding strength f_{yk} =450 N/mm² were used.

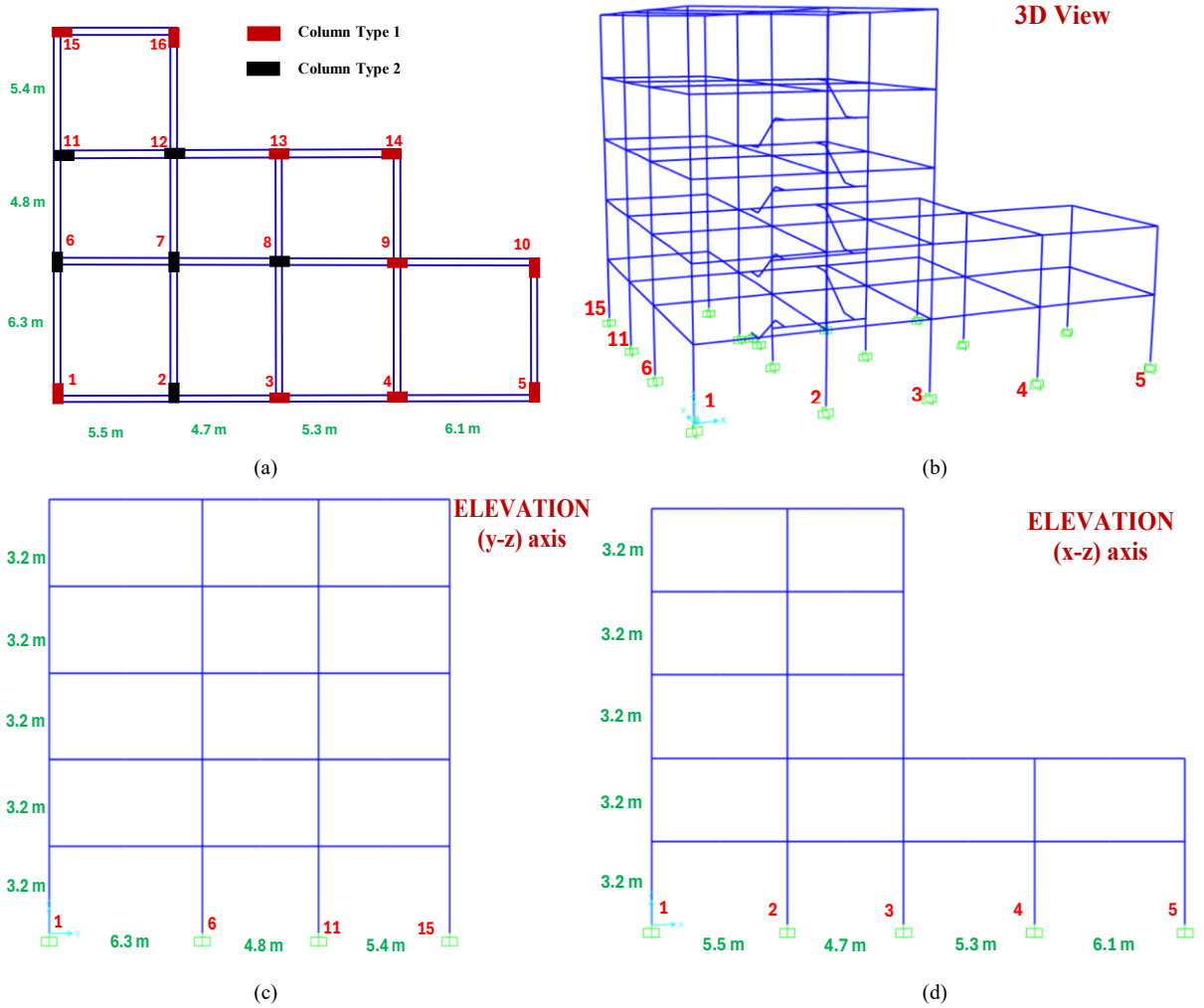

Figure 2: Geometrical details of structure (a) plan; (b) 3-D view; (c) elevation (y-z) axis; (d) elevation (x-z) axis

For a medium ductility design [23], beams were provided with a base width of 300 mm and a height of 600 mm for the first and second floors, and a height of 500 mm for the remaining floors. The plan view in Figure 2(a) illustrates two types of columns, with their dimensions detailed in Table 1(a).

No. of Story	Dimension (cm)	
	Column Type 1	Column Type 2
Story 1	35 x 70	30 x 50
Story 2	30 x 60	30 x 45
Story 3	30 x 50	30 x 40
Story 4	30 x 40	30 x 35
Story 5	30 x 30	30 x 30

Mode	Period	UX	UY	RZ
1	0.836	0.030	0.495	0.224
2	0.823	0.631	0.028	0.012
3	0.651	0.001	0.186	0.350
4	0.357	0.160	0.022	0.111
5	0.343	0.024	0.165	0.022
6	0.326	0.035	0.002	0.178

Table 1: (a) Details of column dimensions; (b) modal mass participant ratios for bare frame

In Table 1(b) the modal mass participation ratios show that, due to the irregularity in elevation, in the first mode in y-direction translational motion is strongly coupled to the rotational motion.

3.1 Bare frame seismic response

Pushover analysis is conducted considering the seismic action along the +X and +Y, and the opposite directions, and the results are shown in Figure (3), where the collapse displacement for each analysis is also reported. The structure has high deformation capacity, reaching structural significant damage limit state in X-direction at displacements of 268 mm (drift=1.67%) and -275mm (drift=1.12%), and 202 mm (drift=1.26%) and -258 mm (drift=1.61%) in the Y-direction, revealing also a smaller base shear strength $V_{bx,max}$=1416 kN in the Y- direction than the base shear strength in the y direction $V_{by,max}$=1122kN.
The structure is able to ensure the performance levels required by the design seismic acceleration, for which the displacement demands in the X and Y directions are 73 mm and 93 mm respectively. Moreover, the drift demand is reported in Table (2) for both the frames that exhibit the maximum and the minimum drift, in order to highlight the influence of torsional behavior.

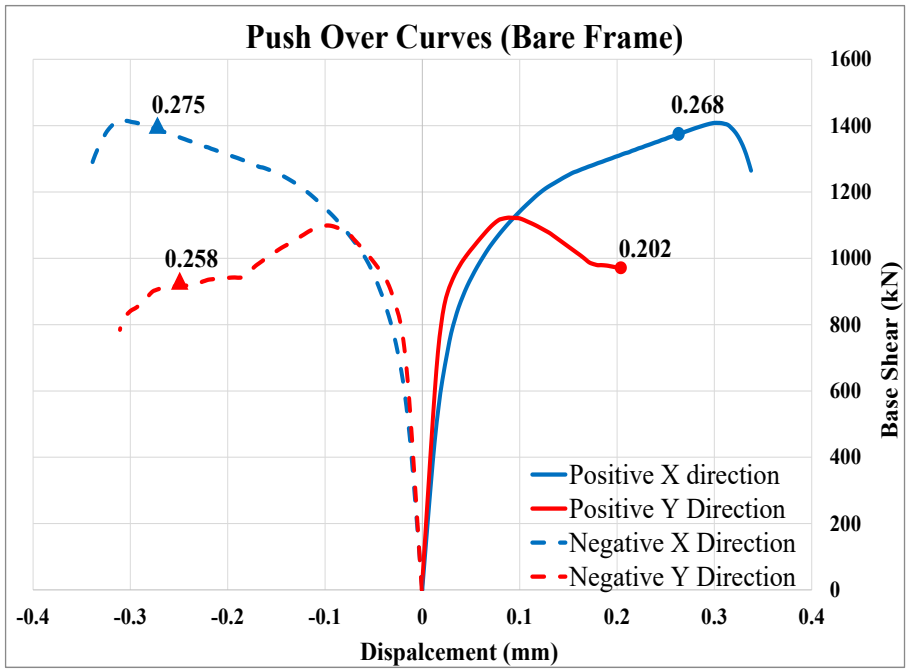

Figure 3: Pushover results of bare frame for both directions

Storey	Demand for return period of 475 years						Structural Significant damage limit state					
	X ($U_{x,CM}$=73 mm)			Y ($U_{y,CM}$=93 mm)			X ($U_{x,CM}$=256 mm)			Y ($U_{y,CM}$=285 mm)		
	D_{max} (%)	D_{min} (%)	Diff. (%)	D_{max} (%)	D_{min} (%)	Diff. (%)	D_{max} (%)	D_{min} (%)	Diff. (%)	D_{max} (%)	D_{min} (%)	Diff. (%)
5	0.38	0.30	23.7	0.39	0.38	0.8	1.85	1.71	8.2	1.53	1.50	2.3
4	0.70	0.59	17.4	0.77	0.72	6.5	2.23	2.13	4.7	2.20	2.12	3.8
3	0.68	0.58	17.9	0.93	1.11	19.9	2.13	2.03	5.1	2.46	2.07	18.7
2	0.41	0.32	28.7	0.74	0.45	64.6	1.68	1.56	7.2	1.57	1.18	33.2
1	0.19	0.16	19.6	0.35	0.22	59.2	1.20	1.06	13.2	0.92	0.63	45.8

Table 2: Bare frame: effect of torsional motion on drift demands for different limit states

The percentage difference between the maximum and minimum drift for each story is also reported. The damage expected can be related to the drift limit values, which according to [46] is 0.5% for brittle infills at the damage limit state, and for ASCE 41-17 [47] are 0.7% for intermediate moment frames for minor damage at immediate occupancy (IO), 1.5% for significant damage life safety limit state (LS), and 2.5% for severe damage at the collapse prevention limit state. The results show that large torsional motion is expected for the design level of PGA, where the difference between the drift in the two external frames due to torsional motion reaches in the Y-direction the 64.6% and 59.2% at the 2nd and 1st story respectively, while in the X-direction are of 28.7% and 19.6% respectively. In accordance with what is well known in the literature, the influence of torsional motion expected for the larger intensity of the seismic excitation according to results derived by pushover analysis, namely at the reaching of the structural significant damage limit state is reduced, with a difference of 45.8% and 33.2% in Y-direction, and 7.2% and 13.2% in X-direction, at the 2nd and 1st story respectively.
Then, increments of the design peak ground acceleration to 0.247 g, or to 0.336 g are considered, due either to an increase in the seismicity of the area or a change in use, resulting in a change in the class of importance and consequently the return period of seismic action. For this level of excitation, roughly an increment of inter-story drifts of more than 40% and 95% are expected, such as not allowing the required performance levels to be guaranteed, especially for the damage limit state. Thus, two retrofitting intervention limiting the inter-story drift to 0.5% are designed in the next section.

3.2 Design of dissipative bracing

The design of strengthening intervention was developed based on the results of the POA, involving the insertion of dissipative bracing to increase frame stiffness in order to limit the damage to the non-structural elements. In the design, two levels of seismic intensity were considered: Significant Damage (SD) with a design PGA of 0.247g, and Near Collapse (NC) with a design PGA of 0.336g, determining a transition from medium to high seismicity. Thus, two different braced frames were designed, which in the following were denoted with the name of the limit state of the design PGA. To determine the bracing characteristics, with the aim of fully exploiting the stiffness and dissipative capacity characteristics provided by the dissipative bracing, the total drift at the design value of the PGA was set equal to 0.5%. Initially, the CAD method was applied in the simplified form [45], aiming at obtaining a uniform drift of 0.5% at each story. Initially, the total area of bracing and the strength required to ensure elastic behavior is evaluated for the two limit states SD and NC; then the strength of the bracing was set equal to 50% of the previously mentioned elastic strength; the results of the procedure are shown in Table (3).

Story No.	Area of bracing (mm^2)				Brace shear strength (50% of elastic strength) (kN)			
	Significant Damage (SD)		Near Collapse (NC)		Significant Damage (SD)		Near Collapse (NC)	
	X	Y	X	Y	X	Y	X	Y
1	6220	8513	19612	19883	1256	1716	3959	4009
2	8722	9399	17518	17742	1720	1895	3537	3577
3	7307	7448	13580	13635	1475	1502	2742	2749
4	5361	5169	9499	9471	1058	1042	1918	1909
5	2116	1982	3905	3774	427	400	789	761

Table 3: Area and shear strength (50% strength required for elastic response) of bracings for SD and NC limit states

The application of the simplified CAD method allowed rational sizing of dissipative bracing, determining the required stiffness and designing effective bracing to improve the building's structural response. During the initial sizing phase, it was decided to distribute two bracings in each direction to each floor, arranging them as centrifuged as possible on two parallel faces and orienting them in opposite directions as shown in Figure (4).

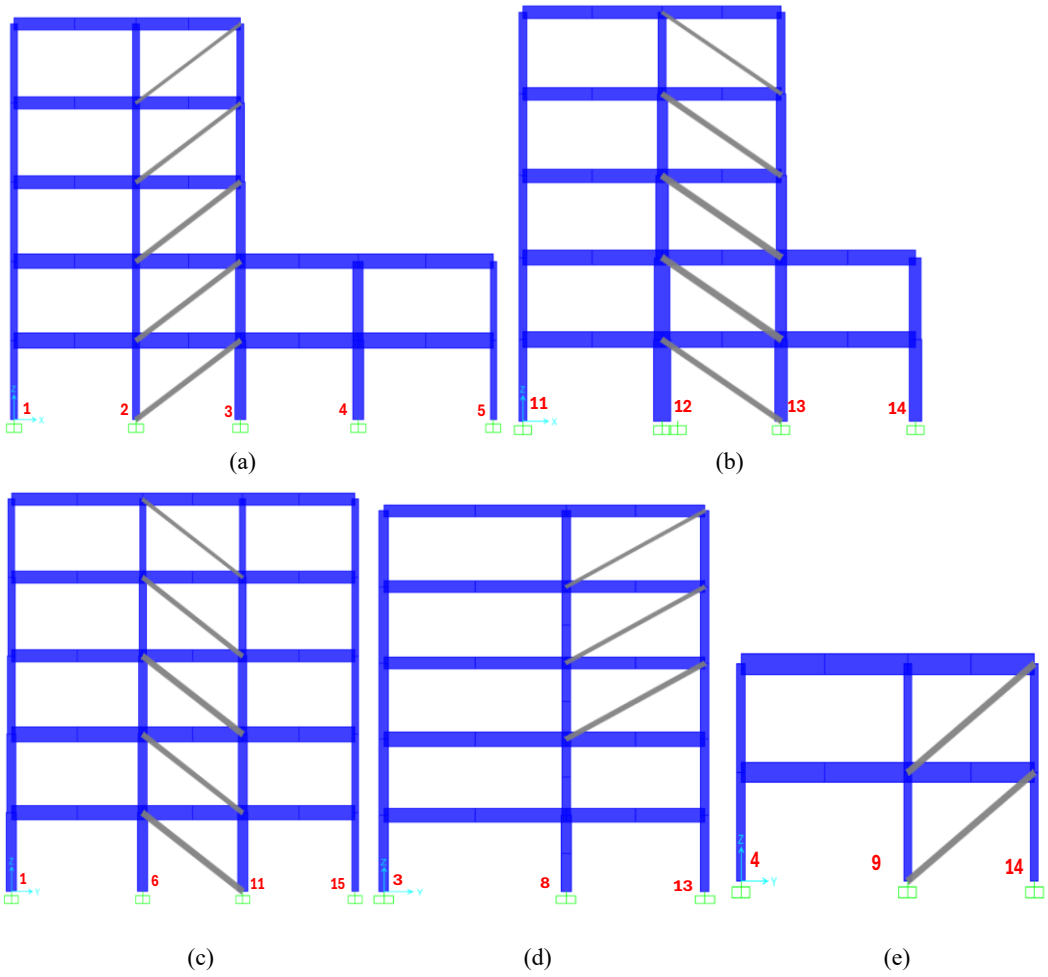

Figure 4: Bracings in elevation X-direction (a) & (b), in Y-direction (c), (d), (e)

The overall stiffness at each floor was distributed on the two faces so that the center of stiffness of the braced structure coincided with the center of application of the seismic floor shear, to eliminate undesirable torsional effects due to geometric irregularity in plan. The profile of the tubular section used to design the braces, having diameter (d) and thickness (s) was chosen to avoid buckling phenomena even if the dissipative device is tuned to ensure elastic behavior up to the design level of PGA acceleration.

The most suitable commercial cross-section was chosen to optimize seismic performance reported below in Table (4) and Table (5) for bracing A and B in the two limit states considered. For the X-direction, Type A bracing was provided in the first frame (1-5) and Type B in the last frame (11-14), while for the Y-direction Type A bracing was provided in the first frame (1-15) and Type B in frame (3-13, 4-14), with the same configuration repeated in height up to the fifth floor. The resistant axial action for each dissipative device was determined by dividing the story shear acting on the brace, proportionally to its area of cross-section, and dividing it by the cosine of its inclination angle of the bay in which the brace is inserted.

Story No.	Bracing A						Bracing B					
	X			Y			X			Y		
	d mm	s mm	A cm²	d mm	s mm	A cm²	d mm	s mm	A cm²	d mm	s mm	A cm²
1	219	4.5	30.3	273	5.6	47.0	244	5	37.6	219	6	40.1
2	219	5	33.6	273	9	74.6	273	6.3	52.7	219	4.5	30.3
3	219	4.5	30.3	273	5	42.0	177	4.5	24.5	219	5	33.6
4	177	4.5	24	219	4.5	30.3	219	5.6	37.5	193	5	29.6
5	139	3.2	13.7	168	4	20.6	159	3.6	17.5	139	3.6	15.3

Table 4: Bracing A and B for SD limit state

Story No.	Bracing A						Bracing B					
	X			Y			X			Y		
	d mm	s mm	A cm²	d mm	s mm	A cm²	d mm	s mm	A cm²	d mm	s mm	A cm²
1	219	12	78.0	267	14.2	112	273	14.2	155	273	11	90.5
2	254	8	61.8	273	8.0	66.6	273	6.5	54.4	229	8	55.5
3	244	6.3	47.1	299	8.8	80.2	244	6.3	47.1	254	8	61.8
4	219	5	33.6	273	6.5	54.4	267	8	65.0	244	6.3	47.1
5	159	3.6	17.5	177	4.5	24.4	219	4.5	30.3	168	4	20.6

Table 5: Bracing A and B for NC limit state

Then, modal analysis was performed on the two braced structures, obtaining the results shown in Table (6) for SD and NC braced frames. Comparison with the corresponding results for the bare frame reported previously in Table 2, shows the reduction of period of vibration in all the modes, the similar stiffness in the two principal directions of the structure, and the increment in torsional stiffness of the structure, proving by the increment of the ratio between period corresponding to larger translational stiffness of the structure (mode 1) T1 and period corresponding to mainly torsional mode (mode 3) T3, that in the bare frame is equal to 1.26, and in the braced frames is 1.38 for SD frame, and 1.41 in the NC frame. Moreover, the strong reduction of the modal mass participation ratio in the torsional motion coupled with the translational modes, that from 22.4% in the bare frame is reduced to 7.1% in the SD braced frame, and to 6.4% in the NC braced frame, proves the effectiveness of the criteria for choosing the in-plane location of the braces. Then, non-linear analysis was performed for both the full strength and 50% strength of the bracing to evaluate the effectiveness of the chosen configuration. The resulting pushover curves are depicted in Figure (5) up to the available deformation capacity of the structures.

MODE	SD braced frame				NC braced frame			
	Period	UX	UY	RZ	Period	UX	UY	RZ
1	0.554	0.310	0.402	0.071	0.461	0.077	0.623	0.064
2	0.541	0.448	0.305	0.018	0.434	0.644	0.089	0.000
3	0.399	0.006	0.057	0.645	0.326	0.009	0.031	0.640
4	0.245	0.000	0.159	0.027	0.214	0.006	0.168	0.030
5	0.241	0.156	0.000	0.000	0.205	0.186	0.003	0.001
6	0.217	0.000	0.001	0.177	0.184	0.000	0.000	0.193

Table 6: Modal mass participation ratios for SD and NC braced frames

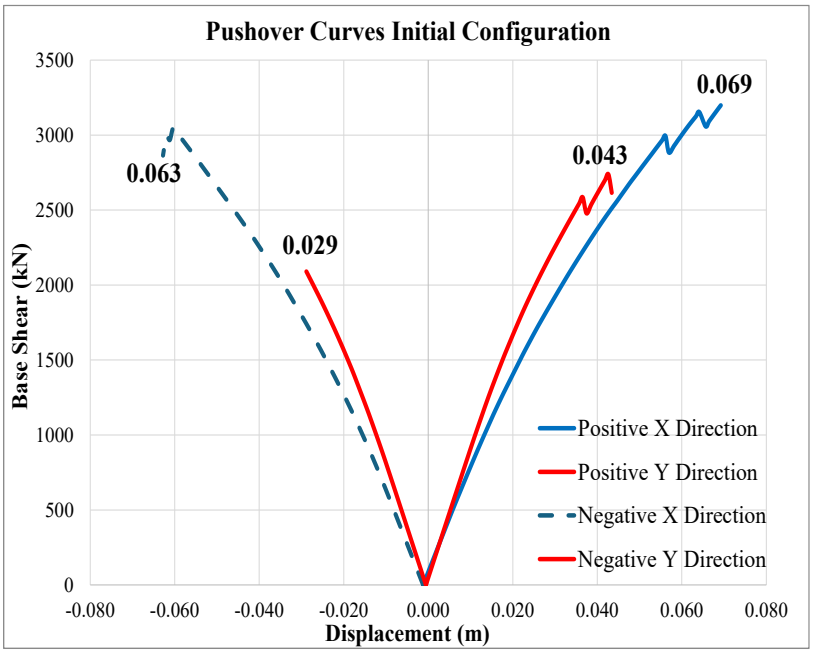

Figure 5: Pushover curve for tentative configuration

It can be noted that the available displacement capacity is strongly reduced, due to variation of the axial force induced by the braces in the column, and the frame is not able to reach the design target displacement equal to 0.08 m. The axial force acting on the columns in the bay with bracing due to Gravity Load (GL) and at the Collapse Displacement (CD) obtained during push-over analysis for displacement in different directions are reported in Table (7) and Table (8). The results show that in each configuration one or more columns are in tension (axial force >0), strongly reducing the available rotation of the plastic hinge.

Story No.	Column 2			Column 3		
	GL	CD $_{Ux<0}$	CD $_{Ux>0}$	GL	CD $_{Ux<0}$	CD $_{Ux>0}$
1	-990	-1982	**439**	-679	**655**	-2678
2	-758	-1360	**88**	-491	**571**	-1972
3	-540	-807	-147	-294	**383**	-1192
4	-323	-373	-291	-173	**143**	-597
5	-110	-82	-125	-57	**26**	-179

Table 7: Pushover analysis: Axial load in negative X and positive X directions for the columns with bracing due to Gravity Load (GL) and at the Collapse Displacement (CD) for the NC braced frame

Story No.	Column 11			Column 6		
	GL	CD $_{Uy<0}$	CD $_{Uy>0}$	GL	CD $_{Uy<0}$	CD $_{Uy>0}$
1	-825	**233**	-2003	-874	-2345	**729**
2	-635	-74	-1252	-681	-1753	**513**
3	-447	-208	-711	-483	-1057	**151**
4	-267	-230	-288	-290	-542	-25
5	-87	-121	-42	-95	-150	-59

Table 8: Pushover analysis: Axial load in negative Y and positive Y directions for the columns with bracing due to Gravity Load (GL) and at the Collapse Displacement (CD) for the NC braced frame

To avoid this undesired behavior, the braces were arranged in different bays, and where this action is not sufficient to avoid the tension action in the column, two braces in the same story of the frame were designed with half of the stiffness and strength of the previous brace each. Thus, the final configuration was obtained shown in Figure (6) and Figure (7).

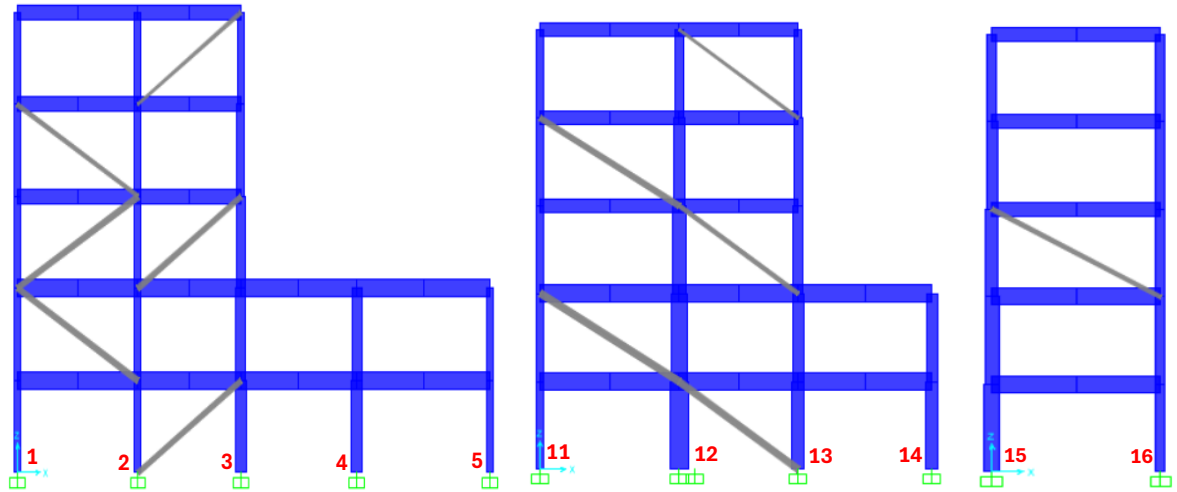

Figure 6: New configuration of bracings in elevation (X-direction)

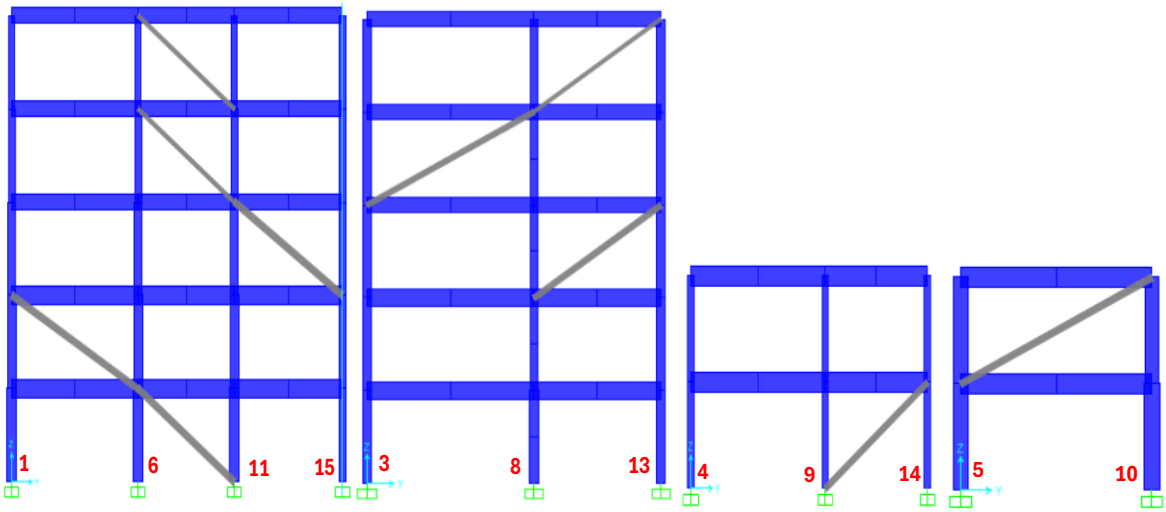

Figure 7: New configuration of bracings in elevation (Y-direction)

3.3 Evaluation of the response of braced structure by Pushover analysis

Nonlinear pushover static analysis was conducted in the X and Y directions to determine the displacement demand for the design earthquake and the deformation capacity of the new configuration of the braced frames. The pushover curves obtained are shown in Figure (8) for the two designed braced frames, together with the displacement demand.

It proves that the design procedure was able to reduce the displacement demand below the target values of 0.08 m, with an exception to the case of action in the negative X-direction for the NC PGA and braced frames configuration, where a slightly larger demand, namely 0.083 m, was found. In all cases, the displacement capacity of the structure is significantly larger than the demand.

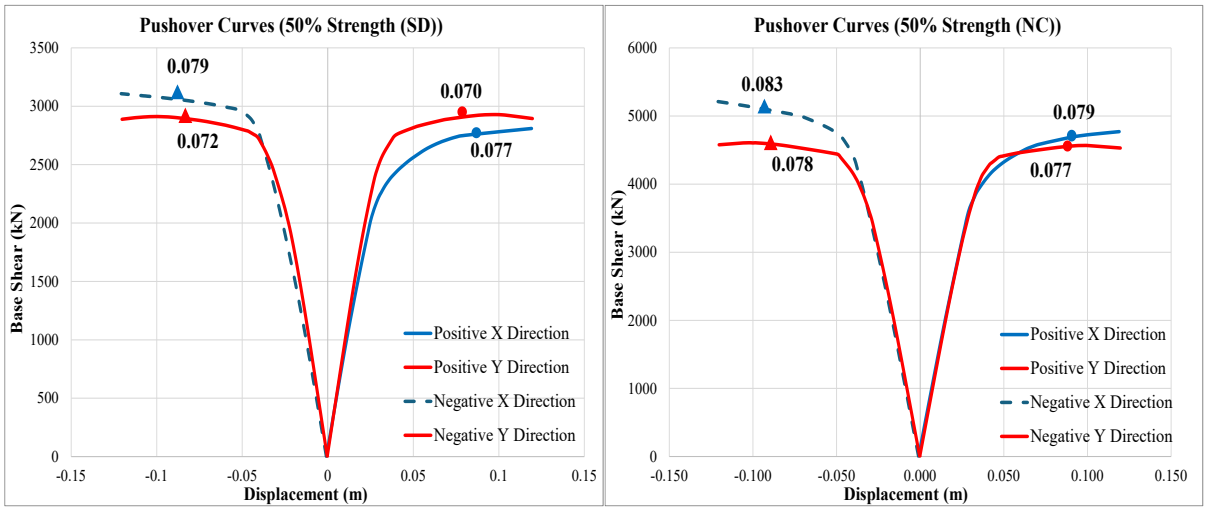

(a) (b)

Figure 8: Pushover curves for 50% of strength (a) significant damage; (b) near collapse

More specifically, for the braced frames designed to withstand the action at the SD limit state, the displacement demand required by the earthquake was 0.083m in the X-direction and 0.078m in the Y-direction, close to that established at the design stage. The analysis carried out for both the collapse limit state and the significant damage limit state, confirmed that the displacement required by the earthquake is less than the ultimate capacity of the structure, ensuring compliance with the seismic verification. Specifically, the structure was found to be capable of reaching a displacement of 120 mm, demonstrating a high deformation capacity. Regarding the NC limit state, in the negative X-direction, the displacement capacity was 0.11 m, with a demand of 0.086 m, while for the positive X-direction, the capacity was 0.090 m, with a demand of 0.081 m. In the negative Y-direction, the displacement capacity of the structure reached 0.13 m, while the demand was 0.081 m. Finally, for positive Y-direction the capacity exhibited was slightly less than 0.12 m, with a demand of 0.08 m. The variation of capacity as a function of earthquake direction shows a slight asymmetry of structural behavior but is still within acceptable limits.

The values of the inter-story drift obtained by pushover analysis for the two structures are shown in Table (9), stressing that with the insertion of the bracings, the damage level of the structure is significantly reduced compared to the initial configuration. For SD braced frame and PGA=0.247 g the target drift is exceeded at the 1st and 2nd story for X-direction of seismic excitation, and 3rd story for Y-direction due to the excessive stiffness of the upper story enforced

Storey	Significant damage limit state SD						Near collapse limit state NC					
	X ($U_{x,CM}$ = 77 mm)			Y ($U_{y,CM}$ = 72 mm)			X ($U_{x,CM}$ = 77 mm)			Y ($U_{y,CM}$ = 72 mm)		
	D_{max} (%)	D_{min} (%)	Diff. (%)	D_{max} (%)	D_{min} (%)	Diff. (%)	D_{max} (%)	D_{min} (%)	Diff. (%)	D_{max} (%)	D_{min} (%)	Diff. (%)
5	0.32	0.29	7.4	0.37	0.33	12.3	0.62	0.60	4.19	0.52	0.47	11.33
4	0.48	0.46	3.4	0.55	0.50	8.7	0.61	0.55	12.00	0.66	0.60	10.99
3	0.50	0.48	5.3	0.62	0.55	11.3	0.53	0.44	20.57	0.62	0.57	9.39
2	0.66	0.59	12.2	0.47	0.44	5.6	0.32	0.31	3.06	0.44	0.43	2.92
1	0.65	0.58	12.4	0.31	0.26	16.7	0.28	0.24	16.88	0.24	0.20	20.00

Table 9: Braced frames: effect of torsional motion on drift demands for SD and NC structures and level of seismic excitation

in the design phase due to the need to use commercial cross-section; the effectiveness of the prediction of the required displacement, combined with the non-uniform distribution of the drift at the different floors, causes the design drift to be exceeded at the floors where no oversizing has been carried out. Moreover, unexpected torsional behavior is still detected for these drifts. For NC braced frame and PGA=0.336 g the detected behavior is characterized by drift larger than the design one at the upper 4th, 5th, and 6th story, maybe due to too much-reduced strength of the dissipative devices, while relevant torsional effects are detected at the 3rd and 1st stories for seismic excitation in the X and Y directions, respectively.

4 NONLINEAR DYNAMIC ANALYSIS

To evaluate the effectiveness of the Push Over Analysis (POA) in predicting the displacements required of the structure by the seismic action, a Nonlinear Time History Analysis (NLTHA) was conducted on the bare and braced frames. Three spettro-compatible artificial accelerograms [48] were applied, with PGA scaled to 0.247g for the SD limit state, and to 0.336g for the NC limit state. The values of the maximum drift for each story and each accelerogram, together with the maxima and mean values, are reported in Table (10) for the bare frame and braced SD frame for PGA=0.247g, and in Table (11) for the bare frame and braced NC frame for PGA=0.336g.

The results for PGA=0.247 show a reduction of the mean value of the drift between all accelerograms and all stories from 0.59% for the bare frame to 0.26% for the SD braced frames, with a reduction of the maximum drift from1.14% obtained at the 4th story for accelerogram #1 for the bare frame to 0.47 obtained at the 2nd story for accelerogram #3 for the SD braced frame. It is noteworthy that the maximum and mean values of drift at the first story of the SD braced frame, namely 0.42% and 0.39% respectively, are larger than the corresponding values for the bare frame, 0.36%, and 0.30% respectively. The results for PGA=0.336g show a reduction of the mean value of the drift between all accelerograms and all stories from 0.72% for the bare frame to 0.41% for the NC braced frames, with a reduction of the maximum drift from 1.33%

Accelerogram. # PGA=0.247 g	Bare Frame					Braced Frame SD				
	Story					Story				
	1	2	3	4	5	1	2	3	4	5
1	0.36	0.60	1.01	1.14	0.68	0.38	0.44	0.23	0.40	0.33
2	0.31	0.50	0.74	0.70	0.37	0.42	0.35	0.18	0.34	0.25
3	0.22	0.35	0.70	0.76	0.48	0.38	0.47	0.23	0.36	0.30
max	0.36	0.6	1.01	1.14	0.68	0.42	0.47	0.23	0.4	0.33
mean	0.30	0.48	0.82	0.87	0.51	0.39	0.42	0.21	0.37	0.29

Table 10: Inter story drift (%) at SD of the unbraced structure and the braced structure with 50% bracing strength

Accelerogram. # PGA=0.336 g	Bare Frame					Braced Frame NC				
	Story					Story				
	1	2	3	4	5	1	2	3	4	5
1	0.45	0.70	1.18	1.33	0.85	0.30	0.20	0.23	0.54	0.45
2	0.44	0.65	0.91	0.86	0.48	0.25	0.19	0.19	0.29	0.28
3	0.28	0.43	0.86	0.91	0.54	0.26	0.22	0.24	0.55	0.45
max	0.45	0.7	1.18	1.33	0.85	0.3	0.22	0.24	0.55	0.45
mean	0.39	0.59	0.98	1.03	0.62	0.27	0.20	0.22	0.46	0.39

Table 11: Inter story drift (%) at NC of the unbraced structure and the braced structure with 100% bracing strength

obtained at the 4th story for accelerogram #1 for the bare frame to 0.45 obtained at the 1st story for accelerogram #1 for the SD braced frame. For this configuration, the unexpected increment of the mean and maximum values of the story drift never occurs.
Lastly, in Table (12) the values of the maximum inter-story deck rotation for each story and each accelerogram, together with the maximum and mean values, are reported for the bare frame and braced SD frame for PGA=0.247 g, and in Table (13) for the bare frame and braced NC frame for PGA=0.336 g.
For the SD braced frames, a reduction of torsional effects due to the bracing of 13% at the 1st story and of 18% at the 2nd story was found, while at the 3rd and 4th story, an increase in the inter-story drift rotation was found, due to the ineffective proportioning of the brace already revealed by pushover analysis.
For the NC braced frame, the efficiency of the procedure is proved by the generalized large reduction of the inter-story drift rotation at each story, which ranges from 91%, 84%, and 86% in the 5th and first two-story, to 63% and 73% in the 3rd and 4th one.

Accelero-gram. # PGA=0.247 g	Bare Frame inter-story deck rotations (x 10^3)					SD Braced Frame inter-story deck rotations (x 10^3)				
	Story					Story				
	1	2	3	4	5	1	2	3	4	5
1	0.152	0.145	0.026	0.133	0.313	0.120	0.100	0.389	0.166	0.144
2	0.144	0.115	0.056	0.057	0.257	0.132	0.116	0.197	0.167	0.164
3	0.134	0.146	0.062	0.130	0.264	0.121	0.117	0.392	0.192	0.155
max	0.152	0.146	0.062	0.133	0.313	0.132	0.117	0.392	0.192	0.164
mean	0.143	0.135	0.048	0.107	0.278	0.124	0.111	0.326	0.175	0.154

Table 12: Rotation at SD of the unbraced structure and the braced structure with 50% bracing strength

Accelero-gram. # PGA=0.336 g	Bare Frame inter-story deck rotations (x 10^3)					NC Braced Frame inter-story deck rotations (x 10^3)				
	Story					Story				
	1	2	3	4	5	1	2	3	4	5
1	0.190	0.180	0.034	0.142	0.239	0.027	0.034	0.027	0.049	0.042
2	0.182	0.134	0.069	0.018	0.197	0.029	0.017	0.029	0.021	0.004
3	0.163	0.115	0.108	0.155	0.145	0.027	0.007	0.023	0.015	0.006
max	0.190	0.180	0.108	0.155	0.239	0.029	0.034	0.029	0.049	0.042
mean	0.178	0.143	0.070	0.105	0.194	0.028	0.019	0.026	0.028	0.017

Table 13: Rotation at NC of the unbraced structure and the braced structure with 50% bracing strength

5 CONCLUSIONS

Criteria and methods for the distribution of stiffnesses and resistances of dissipative bracing both in elevation and in the plan are revised based on the findings in [17,35,44], aiming at reducing structural irregularities, and minimizing the reduction of column deformation capacity due to variation of the axial load.
Thus the following modification of the procedure is suggested: the story stiffness of the bare frame is evaluated by a nonlinear static analysis in which the story displacement is set equal to the target story displacement of the braced structure (i.e. assuming constant inter-story drift and with zero torsional rotation); the stiffness of each braces is evaluated in order to ensure that, at each story, the center of stiffness of the braced frames is coincident with the center of the

seismic story shear, and the maximum torsional stiffness of the frame; the effect of the axial load variation induced by the braces on the ductility of the columns should investigated, and position, number and strength of the braces are modified in order to obtain the smaller reduction or the largest increment of the deformation capacity of the column of the frame.
The procedure was validated for a case study; the results prove the effectiveness of the above-mentioned insights. However, they call for a more accurate choice of the distribution of stiffness and strength of the dissipative braces in plan and in elevation able to take into account the variation in stiffness of the bare frame generated by the variation in the normal stress induced by the bracing, by the variations in stiffness of the bracing required by the use of commercially available sections instead of those suggested by the calculation method, and by unwanted residual effects of the torsional modes that can be triggered during the dynamic response, although not foreseen by the nonlinear static analysis.

6 ACKNOWLEDGEMENT

The studies presented here were carried out as part of the activities envisaged by the RETURN Extended Partnership and received funding from the European Union Next-Generation EU (National Recovery and Resilience Plan—NRRP, Mission 4, Component 2, Investment 1.3—D.D. 1243 2/8/2022, PE0000005).

REFERENCES

1. Gkournelos, P.D.; Triantafillou, T.C.; Bournas, D.A. Seismic Upgrading of Existing Reinforced Concrete Buildings: A State-of-the-Art Review. *Engineering Structures* **2021**, *240*, 112273, doi:10.1016/j.engstruct.2021.112273.
2. Calvi, G.M. Choices and Criteria for Seismic Strengthening. *Journal of Earthquake Engineering* **2013**, *17*, 769–802, doi:10.1080/13632469.2013.781556.
3. De Lorenzis, L.; Teng, J.G. Near-Surface Mounted FRP Reinforcement: An Emerging Technique for Strengthening Structures. *Composites Part B: Engineering* **2007**, *38*, 119–143, doi:10.1016/j.compositesb.2006.08.003.
4. Colajanni, P.; Recupero, A.; Spinella, N. Increasing the Shear Capacity of Reinforced Concrete Beams Using Pretensioned Stainless Steel Ribbons. *Struct Concrete* **2017**, *18*, 444–453, doi:10.1002/suco.201600089.
5. Colajanni, P.; La Mendola, L.; Recupero, A.; Spinella, N. Stress Field Model for Strengthening of Shear-Flexure Critical RC Beams. *J. Compos. Constr.* **2017**, *21*, 04017039, doi:10.1061/(ASCE)CC.1943-5614.0000821.
6. Monti, G.; Liotta, M. Tests and Design Equations for FRP-Strengthening in Shear. *Construction and Building Materials* **2007**, *21*, 799–809, doi:10.1016/j.conbuildmat.2006.06.023.
7. Koutas, L.; Bousias, S.N.; Triantafillou, T.C. Seismic Strengthening of Masonry-Infilled RC Frames with TRM: Experimental Study. *J. Compos. Constr.* **2015**, *19*, 04014048, doi:10.1061/(ASCE)CC.1943-5614.0000507.
8. Golias, E.; Schlüter, F.-H.; Spyridis, P. Strengthening of Reinforced Concrete Beam-Column Joints by Means of Fastened C-FRP Ropes. *Structures* **2024**, *66*, 106811, doi:10.1016/j.istruc.2024.106811.
9. Ebanesar, A.; Gladston, H.; Noroozinejad Farsangi, E.; Sharma, S.V. Strengthening of RC Beam-Column Joints Using Steel Plate with Shear Connectors: Experimental Investigation. *Structures* **2022**, *35*, 1138–1150, doi:10.1016/j.istruc.2021.08.042.

10. Rocca, S.; Galati, N.; Nanni, A. Review of Design Guidelines for FRP Confinement of Reinforced Concrete Columns of Noncircular Cross Sections. *J. Compos. Constr.* **2008**, *12*, 80–92, doi:10.1061/(ASCE)1090-0268(2008)12:1(80).
11. Raza, S.; Khan, M.K.I.; Menegon, S.J.; Tsang, H.-H.; Wilson, J.L. Strengthening and Repair of Reinforced Concrete Columns by Jacketing: State-of-the-Art Review. *Sustainability* **2019**, *11*, 3208, doi:10.3390/su11113208.
12. Colajanni, P.; Papia, M. Hysteretic Behavior Characterization of Friction-Damped Braced Frames. *J. Struct. Eng.* **1997**, *123*, 1020–1028, doi:10.1061/(ASCE)0733-9445(1997)123:8(1020).
13. Akiyama, H. *Earthquake-Resistant Limit-State Design for Buildings*; University of Tokyo press, 1985; ISBN 4-13-068111-7.
14. Colajanni, P.; Recupero, A.; Spinella, N. Shear Strength Degradation Due to Flexural Ductility Demand in Circular RC Columns. *Bull Earthquake Eng* **2015**, *13*, 1795–1807, doi:10.1007/s10518-014-9691-0.
15. Mazza, F. Displacement-Based Seismic Design of Hysteretic Damped Braces for Retrofitting in-Plan Irregular r.c. Framed Structures. *Soil Dynamics and Earthquake Engineering* **2014**, *66*, 231–240, doi:10.1016/j.soildyn.2014.07.001.
16. Di Cesare, A.; Ponzo, F.C. Seismic Retrofit of Reinforced Concrete Frame Buildings with Hysteretic Bracing Systems: Design Procedure and Behaviour Factor. *Shock and Vibration* **2017**, *2017*, 1–20, doi:10.1155/2017/2639361.
17. Ferraioli, M.; Lavino, A. A Displacement-Based Design Method for Seismic Retrofit of RC Buildings Using Dissipative Braces. *Mathematical Problems in Engineering* **2018**, *2018*, 1–28, doi:10.1155/2018/5364564.
18. Bruschi, E.; Quaglini, V.; Calvi, P.M. A Simplified Design Procedure for Seismic Upgrade of Frame Structures Equipped with Hysteretic Dampers. *Engineering Structures* **2022**, *251*, 113504, doi:10.1016/j.engstruct.2021.113504.
19. Benfratello, S.; Caddemi, S.; Palizzolo, L.; Pantò, B.; Rapicavoli, D.; Vazzano, S. Targeted Steel Frames by Means of Innovative Moment Resisting Connections. *Journal of Constructional Steel Research* **2021**, *183*, 106695, doi:10.1016/j.jcsr.2021.106695.
20. Benfratello, S.; Caddemi, S.; Palizzolo, L.; Pantò, B.; Rapicavoli, D.; Vazzano, S. Targeted Steel Frames by Means of Innovative Moment Resisting Connections. *Journal of Constructional Steel Research* **2021**, *183*, 106695, doi:10.1016/j.jcsr.2021.106695.
21. Barbagallo, F.; Bosco, M.; Marino, E.M.; Rossi, P.P.; Stramondo, P.R. A Multi-performance Design Method for Seismic Upgrading of Existing RC Frames by BRBs. *Earthq Engng Struct Dyn* **2017**, *46*, 1099–1119, doi:10.1002/eqe.2846.
22. Pagnotta, S.; Ahmed, M.; Colajanni, P. Experimental and Finite Element Analysis of the Cyclic Behaviour of Linear Dissipative Devices. In *COMPDYN Proceedings*; National Technical University of Athens, 2023.
23. Colajanni, P.; La Mendola, L.; Monaco, A.; Pagnotta, S. Dissipative Connections of Rc Frames with Prefabricated Steel-Trussed-Concrete Beams. *Ingegneria Sismica* **2020**, *37*, 51–63.
24. Titirla, M.D. A State-of-the-Art Review of Passive Energy Dissipation Systems in Steel Braces. *Buildings* **2023**, *13*, 851, doi:10.3390/buildings13040851.
25. Yoo, J.-H.; Lehman, D.E.; Roeder, C.W. Influence of Connection Design Parameters on the Seismic Performance of Braced Frames. *Journal of Constructional Steel Research* **2008**, *64*, 607–623, doi:10.1016/j.jcsr.2007.11.005.
26. Valente, M.; Milani, G. Alternative Retrofitting Strategies to Prevent the Failure of an Under-Designed Reinforced Concrete Frame. *Engineering Failure Analysis* **2018**, *89*, 271–285, doi:10.1016/j.engfailanal.2018.02.001.

27. Filiatrault, A.; Cherry, S. Seismic Design Spectra for Friction-Damped Structures. *J. Struct. Eng.* **1990**, *116*, 1334–1355, doi:10.1061/(ASCE)0733-9445(1990)116:5(1334).
28. Ciampi, V. Development of Passive Energy Dissipation Techniques for Buildings. In Proceedings of the Proceedings International Post-SMIRT Conference Seminar on Isolation, Energy Dissipation and Control of Vibrations of Structures; 1993; pp. 495–510.
29. Constantinou, M.C.; Soong, T.T.; Dargush, G.F. Passive Energy Dissipation Systems for Structural Design and Retrofit. **1998**.
30. Maison, B.F.; Popov, E.P. Cyclic Response Prediction for Braced Steel Frames. *J. Struct. Div.* **1980**, *106*, 1401–1416, doi:10.1061/JSDEAG.0005464.
31. Mazza, F.; Vulcano, A. Displacement-Based Design Procedure of Damped Braces for the Seismic Retrofitting of r.c. Framed Buildings. *Bull Earthquake Eng* **2015**, *13*, 2121–2143, doi:10.1007/s10518-014-9709-7.
32. Amadio, C.; Fragiacomo, M.; Rajgelj, S. The Effects of Repeated Earthquake Ground Motions on the Non-linear Response of SDOF Systems. *Earthq Engng Struct Dyn* **2003**, *32*, 291–308, doi:10.1002/eqe.225.
33. Lin, Y.Y.; Tsai, M.H.; Hwang, J.S.; Chang, K.C. Direct Displacement-Based Design for Building with Passive Energy Dissipation Systems. *Engineering Structures* **2003**, *25*, 25–37, doi:10.1016/S0141-0296(02)00099-8.
34. Mazza, F.; Vulcano, A. Equivalent Viscous Damping for Displacement-Based Seismic Design of Hysteretic Damped Braces for Retrofitting Framed Buildings. *Bull Earthquake Eng* **2014**, *12*, 2797–2819, doi:10.1007/s10518-014-9601-5.
35. Ferraioli, M.; Lavino, A.; Molitierno, C.; Di Lauro, G. Seismic Retrofit of an Existing Reinforced Concrete Building with Buckling-Restrained Braces. *TOCIEJ* **2021**, *15*, 203–225, doi:10.2174/1874149502115010203.
36. CSLLPP *Istruzioni per l'applicazione Dell'«Aggiornamento Delle "Norme Tecniche per Le Costruzioni"» Di Cui al Decreto Ministeriale 17 Gennaio 2018, Roma; 2019, in Italian*; **2019**.
37. Shibata, A.; Sozen, M.A. Substitute-Structure Method for Seismic Design in R/C. *J. Struct. Div.* **1976**, *102*, 1–18, doi:10.1061/JSDEAG.0004250.
38. Elishakoff, I.; Colajanni, P. Stochastic Linearization Critically Re-Examined. *Chaos, Solitons & Fractals* **1997**, *8*, 1957–1972, doi:10.1016/S0960-0779(97)00035-0.
39. Maulana, T.I.; Fonseca, P.A.D.F.; Saito, T. Application of Genetic Algorithm to Optimize Location of BRB for Reinforced Concrete Frame with Curtailed Shear Wall. *Applied Sciences* **2022**, *12*, 2423, doi:10.3390/app12052423.
40. Laguardia, R.; Franchin, P. Risk-Based Optimization of Bracing Systems for Seismic Retrofitting of RC Buildings. *J. Struct. Eng.* **2022**, *148*, 04022049, doi:10.1061/(ASCE)ST.1943-541X.0003335.
41. Franchin, P.; Petrini, F.; Mollaioli, F. Improved Risk-targeted Performance-based Seismic Design of Reinforced Concrete Frame Structures. *Earthq Engng Struct Dyn* **2018**, *47*, 49–67, doi:10.1002/eqe.2936.
42. Mazza, F.; Mazza, M.; Vulcano, A. Displacement-Based Seismic Design of Hysteretic Damped Braces for Retrofitting in-Elevation Irregular r.c. Framed Structures. *Soil Dynamics and Earthquake Engineering* **2015**, *69*, 115–124, doi:10.1016/j.soildyn.2014.10.029.
43. Antoniou, S. Development and Verification of a Displacement-Based Adaptive Pushover Procedure. *J. Earth. Eng.* **2004**, *8*, 643, doi:10.1142/S136324690400150X.
44. Ferraioli, M.; Pecorari, O.; Farace, D.; Di Lauro, G. Influence of Torsional Effects in Seismic Retrofit of RC Buildings. *Procedia Structural Integrity* **2024**, *64*, 1017–1024, doi:10.1016/j.prostr.2024.09.430.

45. Colajanni, P.; Ahmed, M.; D'Anna, J. Comparison between Design Methods for Seismic Retrofit of Reinforced Concrete Frames Using Dissipative Bracing Systems. *Buildings* **2024**, *14*, 3256, doi:10.3390/buildings14103256.
46. EN 1998–1 *Design of Structures for Earthquake Resistance - Part 1: General Rules, Seismic Actions and Rules for Buildings, CEN*; **2005**.
47. *ASCE Standard, ASCE/SEI, 41-17: Seismic Evaluation and Retrofit of Existing Buildings*; Structural Engineering Institute, Structural Engineering Institute, American Society of Civil Engineers, Eds.; American Society of Civil Engineers: Reston, Virginia, 2017; ISBN 978-0-7844-1485-9.
48. Cacciola, P.; Colajanni, P.; Muscolino, G. Combination of Modal Responses Consistent with Seismic Input Representation. *J. Struct. Eng.* **2004**, *130*, 47–55, doi:10.1061/(ASCE)0733-9445(2004)130:1(47).